

# Asymmetric Amination of Unstrained C(sp<sup>3</sup>)–C(sp<sup>3</sup>) Bonds

Yang Liu, Ye-Wei Chen, Yuan-Xiang Yang, John F. Hartwig,\* and Zhi-Tao He\*



Cite This: *J. Am. Chem. Soc.* 2024, 146, 29857–29864



Read Online

ACCESS |

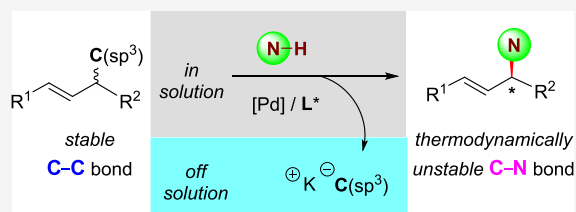
Metrics & More

Article Recommendations

Supporting Information

**ABSTRACT:** The asymmetric functionalization of unstrained C(sp<sup>3</sup>)–C(sp<sup>3</sup>) bonds could be a powerful strategy to stereoselectively reconstruct the backbone of an organic compound, but such reactions are rare. Although allylic substitutions have been used frequently to construct C–C bonds by the cleavage of more reactive C–X bonds (X is usually an O atom of an ester) by transition metals, the reverse process that involves the replacement of a C–C bond with a C–heteroatom bond is rare and generally considered thermodynamically unfavorable. We show that an unstrained, inert allylic C–C  $\sigma$  bond can be converted to a C–N bond stereoselectively via a designed solubility-control strategy,

which makes the thermodynamically unfavorable process possible. The C–C bond amination occurs with a range of amine nucleophiles and cleaves multiple classes of alkyl C–C bonds in good yields with high enantioselectivity. A novel resolution strategy is also reported that transforms racemic allylic amines to the corresponding optically active allylic amine by the sequential conversion of a C–N bond to a C–C bond and back to a C–N bond. Mechanistic studies show that formation of the C–N bond is the rate-limiting step and is driven by the low solubility of the salt formed from the cleaved alkyl group in a nonpolar solvent.



## INTRODUCTION

The ubiquity of saturated C–C bonds in organic molecules makes the selective functionalization of such bonds an approach that could change and make more efficient synthetic strategies.<sup>1–11</sup> However, the kinetic and thermodynamic challenges that confront the mild cleavage of C(sp<sup>3</sup>)–C(sp<sup>3</sup>) bonds make reactions at these positions of molecules rare. Even less common are enantioselective reactions at such bonds. Most reported enantioselective reactions occurring at C(sp<sup>3</sup>)–C(sp<sup>3</sup>) bonds arise from strain release of small rings.<sup>12–34</sup> One report by Zhu et al. described a catalytic process occurring through a rearrangement step and included a single example of enantioselective cleavage of an unstrained C(sp<sup>3</sup>)–C(sp<sup>3</sup>) bond with high selectivity, but this reaction occurred in only 27% yield.<sup>35</sup> Recently, Zuo et al. described the deracemization of unstrained alcohols by Ti-catalyzed, photochemical cleavage and reformation of C–C  $\sigma$  bonds, but focused on the use of special structures and did not introduce a new bond (Scheme 1A, left).<sup>36</sup> Up to now, a protocol to convert inert C–C  $\sigma$  bonds into thermodynamically less stable C–heteroatom bonds stereoselectively remains undeveloped (Scheme 1A, right).

Asymmetric allylic substitution catalyzed by transition-metal complexes has become a common transformation in organic synthesis.<sup>37–51</sup> Generally, a carbon–oxygen bond vicinal to an alkene unit cleaves to release a leaving group and form the critical allyl metal intermediate. The inherent inertness of a C–C bond and relatively high reactivity of C–heteroatom bonds toward transition metals causes conventional studies of this process to focus on the conversion of allylic C–O bonds into allylic C–C bonds (Scheme 1B). Although a few prior studies

revealed the cleavage of unstrained allylic C–C bonds, no C–heteroatom bond was constructed from these reactions, and no stereocenter was introduced at the allylic position.<sup>52–57</sup> If this general sequence for reactions at allylic C–C bonds could be reversed, then one could cleave unstrained allylic C–C bonds to form C–heteroatom bonds and broaden the scope of C–C bonds that can be considered to be reactive positions of organic molecules.

Recently, we reported the stereoselective replacement of one allylic C–C bond by another C(sp<sup>3</sup>)–C(sp<sup>3</sup>) bond by a Pd-catalyzed kinetic resolution and a Pd-catalyzed dynamic kinetic asymmetric transformation.<sup>58</sup> The driving force for this exchange of C–C bonds resulted from the difference in thermodynamic stability of the anionic form of the carbon-based nucleophile and the carbon-based leaving group. However, we were unable to achieve the enantioselective synthesis of a C–X (X = heteroatom) bond from a C–C bond by this strategy due to the unfavorable stability of the respective leaving groups and nucleophile. We envisioned that continuous removal of the carbon-based leaving group from the reaction solution could enable the formation of C–X bond from a C–C bond (Scheme 1C).

We report the realization of this strategy as an asymmetric amination that occurs by the cleavage of a C(sp<sup>3</sup>)–C(sp<sup>3</sup>)

**Received:** August 27, 2024

**Revised:** October 9, 2024

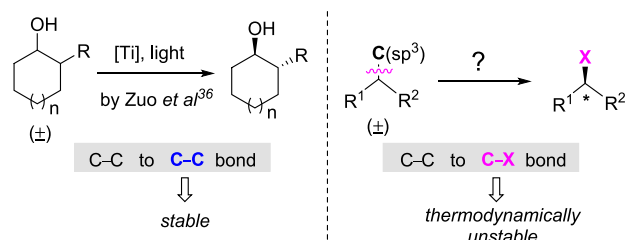
**Accepted:** October 10, 2024

**Published:** October 16, 2024

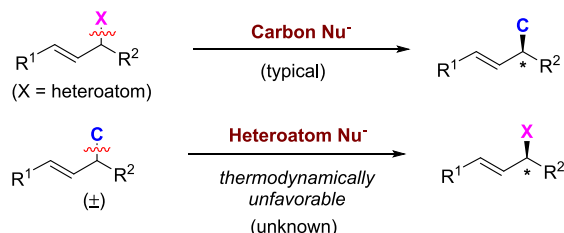


### Scheme 1. Asymmetric C(sp<sup>3</sup>)-C(sp<sup>3</sup>) Bond Functionalization and Our Strategy

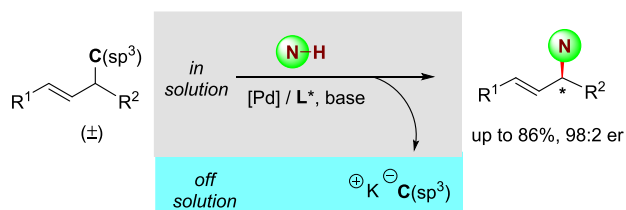
#### A Asymmetric C(sp<sup>3</sup>)-C(sp<sup>3</sup>) bond cleavage



#### B Conventional allylic substitution



#### C This work: C(sp<sup>3</sup>)-C(sp<sup>3</sup>) bond amination

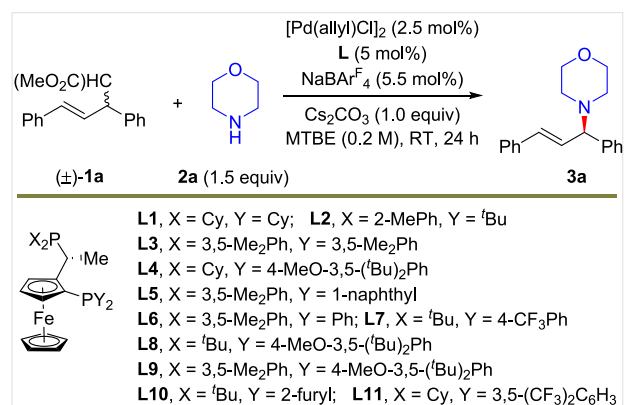


bond and the removal of the carbon-based leaving group. This protocol enables the replacement of an inert C–C  $\sigma$  bond by the C–N bond to a variety of amines, including primary amines, secondary amines, and *N*-heteroaryl amines in moderate to good yield and with high enantioselectivity. Even a mixture of four stereoisomers of the starting alkenes is converted into a single stereoisomer by this C–C bond amination. This strategy, combined with typical allylation, also provides a novel resolution of racemic allylic amines to a single corresponding enantiomer. Mechanistic studies show that formation of the C–N bonds is likely the turnover-limiting step and is driven by the low solubility of the cleaved carbon salt in nonpolar arene solvents.

## RESULTS AND DISCUSSION

**Reaction Development.** We initiated studies of the C–C bond amination by conducting reactions with racemic **1a** bearing a malonate as a carbon leaving group and morpholine **2a** as the nucleophile, inorganic Cs<sub>2</sub>CO<sub>3</sub> as the base, and MTBE as the solvent with a palladium catalyst. A set of chiral JosiPhos-type bisphosphines were evaluated first as the ligand on palladium (Table 1, entries 1–11). The reaction with **L1** as the ligand formed the expected allylic amination product **3a** in 37% yield but with no enantioselectivity (entry 1). Reactions with catalysts containing other JosiPhos ligands provided similar results with varying yields and enantioselectivities (less than 81:19 er, entries 2–10 and see SI for more details) of **3a**. The reaction with **L11** formed **3a** in only 10% yield, but it did occur with a high 94:6 er (entry 11). Increasing the amount of nucleophile **2a** increased the conversion to form **3a** in 22% yield with 95:5 er (entry 12).

### Table 1. Reaction Development for Asymmetric C–C Amination



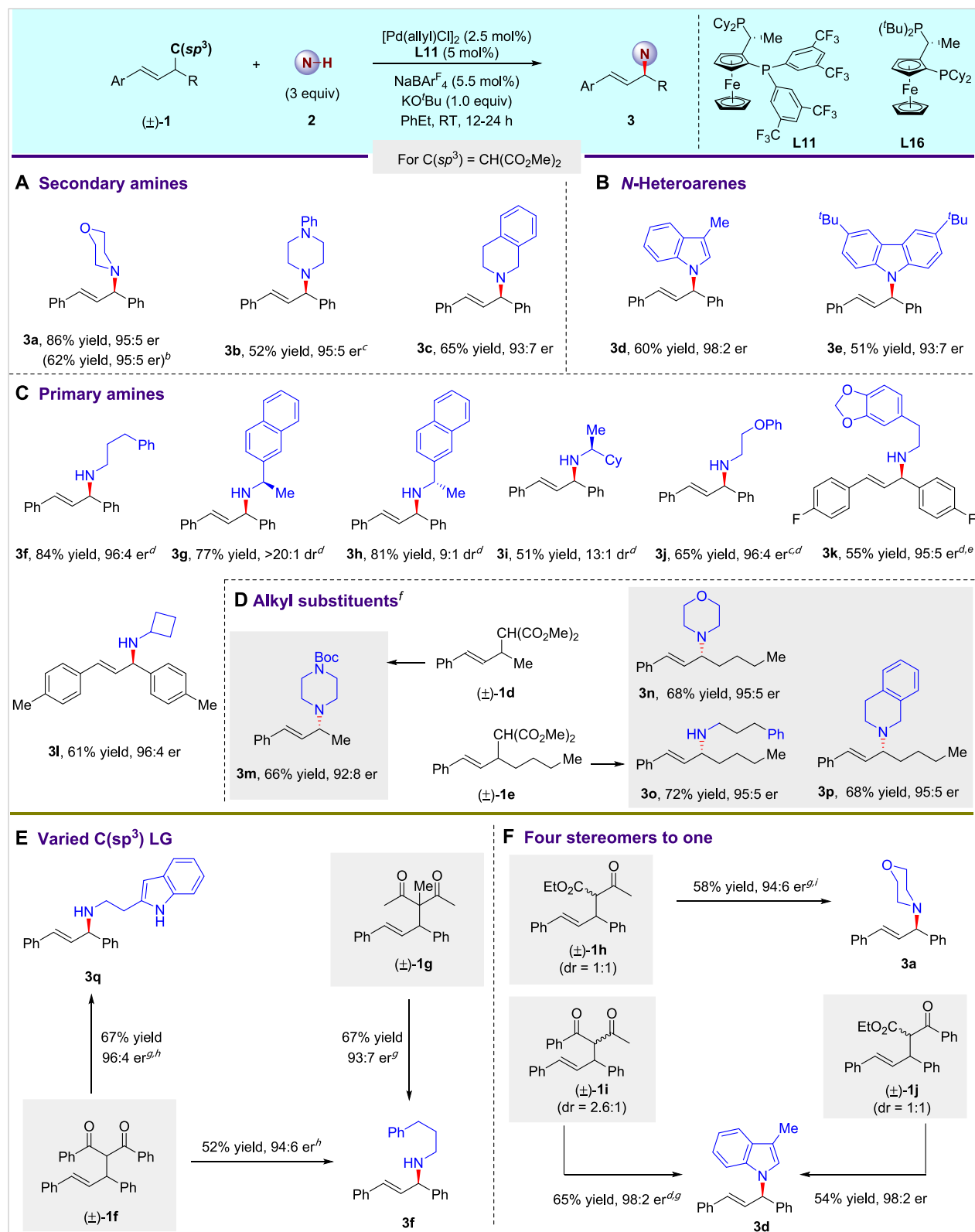
Entry <sup>a</sup>	L	Solvent	Yield (%)	er
1	L1	MTBE	37	50:50
2	L2	MTBE	4	55:45
3	L3	MTBE	10	30:70
4	L4	MTBE	32	75:25
5	L5	MTBE	34	19:81
6	L6	MTBE	30	72:28
7	L7	MTBE	41	69:31
8	L8	MTBE	76	40:60
9	L9	MTBE	12	75:25
10	L10	MTBE	72	58:42
11	L11	MTBE	10	94:6
12	L11	MTBE	22	95:5
13	L11	cyclohexane	61	90:10
14	L11	mesitylene	69	82:18
15	L11	MeOH	18	53:47
16 <sup>b</sup>	L11	PhEt	56	91:9
17 <sup>b,c</sup>	L11	PhEt	86	95:5

<sup>a</sup>The reaction was carried out in 0.10 mmol scale. The yield was determined by <sup>1</sup>H NMR. The er was determined by HPLC analysis.

<sup>b</sup>**2a** (3 equiv) was used. <sup>c</sup>PhEt (0.5 M) was used as the solvent.

<sup>d</sup>KO<sup>t</sup>Bu was used instead of Cs<sub>2</sub>CO<sub>3</sub>. Isolated yield.

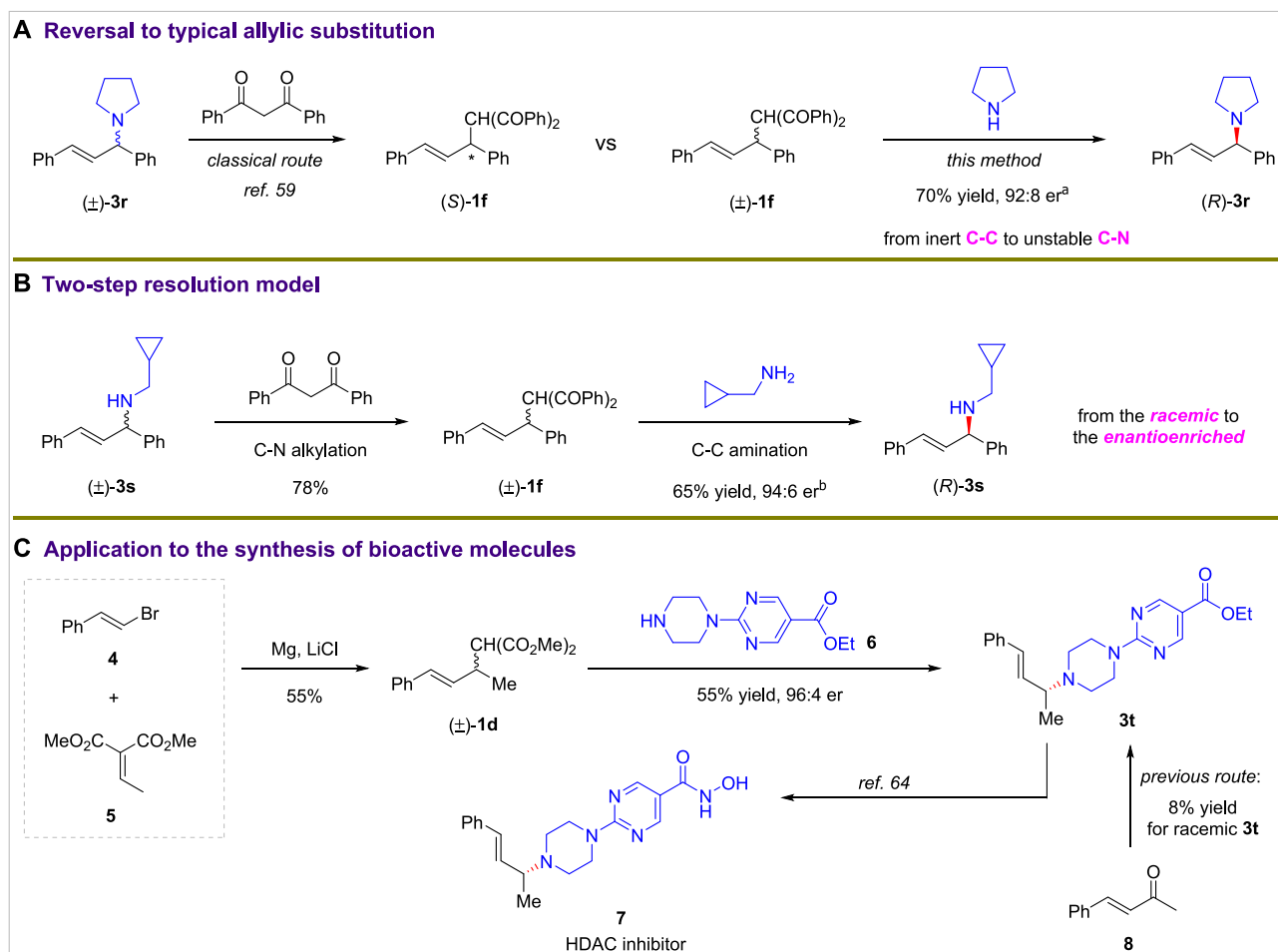
Because the cleaved malonate leaving group is also a nucleophile and the allylic C–C bond is thermodynamically more stable than the allylic C–N bond, the formation of a C–C bond over the C–N bond by the allyl intermediate is favored and accounts for the low yields.<sup>59–63</sup> For this reason, we considered that a strategy to override the thermodynamic preferences by controlling the concentrations might provide a solution to this challenge. A reduction in the solvent polarity could reduce the solubility of the malonate salt produced by the reaction, thereby favoring the amination process. Thus, we conducted the reaction in several nonpolar solvents and found that the yield of **3a** increased to over 60% in both cyclohexane and mesitylene solvents with only a slight erosion of enantioselectivity (entries 13–14). In contrast, reactions in MeOH as a solvent generated **3a** in only 18% yield (entry 15). The reaction in MeOH also occurred with low enantioselectivity, presumably because of the facile racemization of the allylic amine product in protic solvents in the presence of the palladium catalyst. Ultimately, the reaction in ethylbenzene provided **3a** in good yield and with good er (entry 16), and reactions with different bases (see Supporting Information for details) showed that those with KO<sup>t</sup>Bu as base formed **3a** in 86% yield and with 95:5 er (entry 17).

Scheme 2. Scope for C–C  $\sigma$  Bond Amination<sup>a</sup>

<sup>a</sup>Isolated yield. The ee was determined by HPLC analysis. <sup>b</sup>Morpholine **2a** (1.0 equiv) as the nucleophile was used. <sup>c</sup>[Pd(allyl)Cl]<sub>2</sub> (4 mol %), L11 (8.8 mol %), NaBARF<sub>4</sub> (8.8 mol %), and **2** (5 equiv) were used. <sup>d</sup>*p*-Xylene was used as the solvent. <sup>e</sup>Pd(allyl)Cl<sub>2</sub> (4 mol %), L11 (8.8 mol %), and NaBARF<sub>4</sub> (8.8 mol %) were used. <sup>f</sup>Nucleophile (1.0 equiv), electrophile (2.0 equiv), and ligand L16 were used. See SI for more detailed conditions. <sup>g</sup>Cs<sub>2</sub>CO<sub>3</sub> was used. <sup>h</sup>The reaction temperature was 0 °C. <sup>i</sup>**2** (5 equiv) was used.

**Scope of the Unstrained C–C  $\sigma$  Bond Amination.**  
Having identified conditions for enantioselective C–C bond

amination in high yield and er, the scope of the reaction was examined, and the results are summarized in Scheme 2. A

Scheme 3. Applications of C–C  $\sigma$  Bond Amination<sup>a</sup>

<sup>a</sup>See the [Supporting Information](#) for detailed reaction conditions. Isolated yield. The er was determined by HPLC analysis.

series of secondary amines, including morpholine, piperazine, and tetrahydroisoquinoline, underwent the C–C bond amination smoothly, affording the corresponding products **3a–3c** in 52–86% yield and 93:7–95:5 er ([Scheme 2A](#)). An excess of amine as nucleophile was not always necessary. The reaction with 1.0 equiv of morpholine **2a** at the allylic C–C bond formed **3a** in a yield (62%) that was only slightly lower than that with 3.0 equiv and with the same 95:5 er. The reaction also occurred with N–H bonds of aromatic heterocycles to form the corresponding amination products **3d–3e** in reasonable yields and with good enantioselectivity ([Scheme 2B](#)). In addition, a set of primary amines containing arenes, ethers, acetals, and small rings reacted to replace the malonate moiety in the alkenes and form the corresponding chiral allylic amines in moderate to good yields and with high enantioselectivities ([Scheme 2C](#), **3f–3l**).

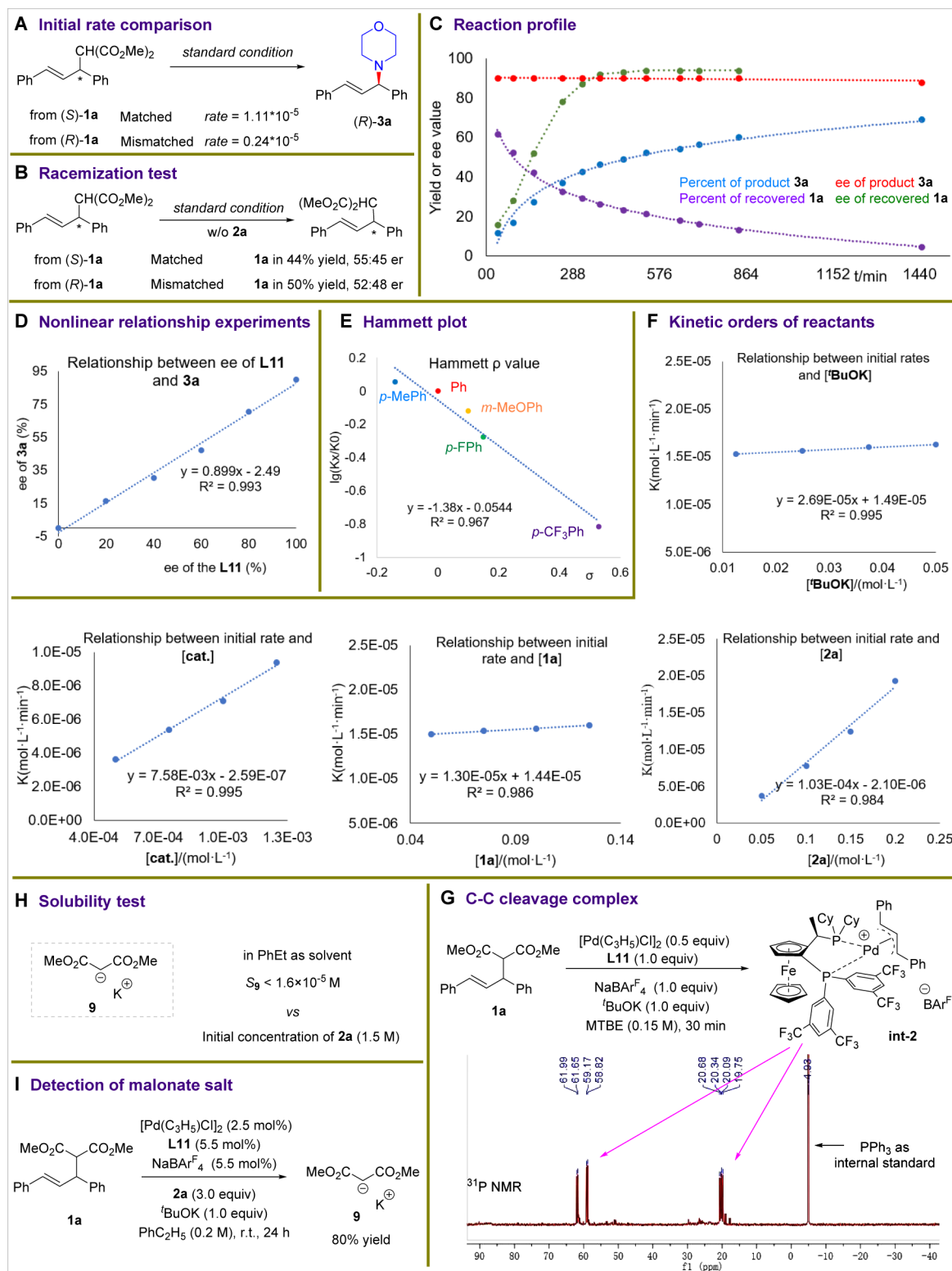
In addition to these diaryl-substituted alkene electrophiles, a series of unsymmetric arylalkyl-substituted alkenes were suitable for C–C bond amination ([Scheme 2D](#), **3m–3p**). In this case, two equivalents of alkene were required to guarantee the observation of reasonable yields for the transformation. For example, with the unsymmetric racemic alkene **1e** as the electrophile, product **3o** was prepared smoothly in 72% yield with 95:5 er by this C–C  $\sigma$ -bond functionalization. When an alkene bearing two aryl substituents featuring different electronic characters was used as the substrate, the

regioselectivity of corresponding allylation favored the site vicinal to the electron-deficient group, but the related enantioselectivity was difficult to be controlled (see [Supporting Information](#) for details).

In addition to alkenes containing a malonate group, alkenes bearing other 1,3-dicarbonyl groups (**1f**, **1g**) underwent aminations at the allylic C–C bond ([Scheme 2E](#)). A nucleophile containing an amine and a heteroaryl N–H bond reacted exclusively at the amine to form product **3q** in 67% yield with 96:4 er. As observed with malonate nucleophiles, a racemic mixture of all four stereoisomers of substrate **1h** reacted with an amine to form one enantiomer of chiral amine **3a** with high stereoselectivity ([Scheme 2F](#)). This conversion of four stereoisomers into one was further highlighted by the conversion of two additional diastereomeric mixtures (**1i** and **1j**) to form the same amination product **3d** in around 60% yield with 98:2 er. The similarly high enantioselectivity of **3d** from reactions at different allylic C–C bonds (**1a**, **1i**, and **1j**) indicates that the same allyl-Pd intermediate forms without the involvement of the cleaved alkyl nucleophiles.

To illustrate the value of this alkyl C–C bond amination reaction in synthetic applications, a series of transformations shown in [Scheme 3](#) were conducted. First, the aminations of alkyl C–C bonds were run in the opposite direction as reactions that form C–C bonds from C–N bonds. The

## Scheme 4. Mechanistic Studies



optically active compound **1f** was previously prepared from allylic amine **3r** by the Tsuji-Trost reaction.<sup>59</sup> Now, by our protocol, the reverse reaction forms the C–N bond in **3r** by cleavage of the C–C bond in **1f** (Scheme 3A). Second, we developed a protocol to transform racemic allyl amines into enantioenriched versions of the same amine by a two-step resolution. For example, *rac*-**3s** was converted into *rac*-**1f** by

allylic substitution and then subject to asymmetric C–C bond amination to regenerate **3s**, but in highly enantioenriched form (Scheme 3B). Third, this asymmetric C–C bond cleavage can facilitate the synthesis of medically relevant compounds. For example, as shown in Scheme 3C, a histone deacetylase (HDAC) inhibitor was prepared by a two-step sequence in which the substrate for asymmetric C–C bond functionaliza-

tion *rac*-**1d** was prepared from alkenyl halide **4** and unsaturated carbonyl ester **5** by Michael addition, and subsequent asymmetric amination at the C–C bond led to the generation of **3t**, which was converted to the enantioenriched HDAC inhibitor **7**.<sup>64</sup> Previously, **3t** was prepared in only 8% yield and in racemic form from enone **8**.<sup>64</sup>

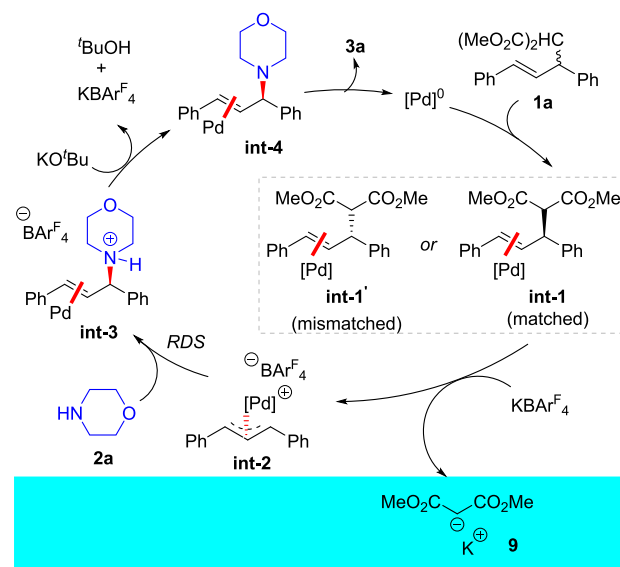
**Preliminary Mechanistic Studies.** To gain experimental information about the mechanism of this C–C bond amination, a series of studies were conducted (Scheme 4). First, the initial rates for the reactions of enantioenriched electrophile **1a** with morpholine **2a** under the standard conditions were measured. The initial rate of the transformation of matched allyl malonate (*S*)-**1a** to form the product (*R*)-**2a** is about 4.6-times faster than that of the mismatched malonate (*R*)-**1a** (Scheme 4A), suggesting that both enantiomers of **1a** are readily converted to product **3a**. Meanwhile, when enantioenriched (*S*)- and (*R*)-**1a** were exposed to the catalyst without nucleophile **2a**, both enantiomers racemized (Scheme 4B). These results indicate that the amination occurs by an identical  $\pi$ -allyl-Pd intermediate. A full profile of the model reaction between racemic **1a** and amine **2a** for the preparation of enantioenriched **3a** also was obtained and is shown in Scheme 4C. The ee of unreacted substrate **1a** increased with the consumption of **1a**, while the ee of product **3a** was nearly constant during the reaction. These data indicate that both matched and mismatched isomers of **1a** react by identical enantiodetermining transition states.

Experiments to probe a relationship between the enantioselectivity of **L11** and that of product **3a** showed that the relationship was within experimental error of linear. This result implies that the reaction occurs with a mononuclear Pd and a chiral ligand as the catalyst (Scheme 4D). The slope of a Hammett plot in Scheme 4E that reveals the effect of the electronic properties of the aryl group in the alkene electrophile on the reaction was negative ( $\rho = -1.38$ ), indicating that a positive charge accumulates in the allyl group in the intermediate. In addition, the kinetic orders of reactants, catalyst, and base (Scheme 4F) showed that the reaction is first order in the nucleophile **2a** and catalyst, but zero order in the electrophile **1a** and base. These data imply that the step that forms the amine product from reaction of the Pd-allyl intermediate and the neutral amine nucleophile **2a** is rate determining. To further support the C–C activation process, the alkene substrate **1a** was treated with 1.0 equiv of the palladium catalyst (Scheme 4G). The in situ <sup>31</sup>P NMR spectra showed that the expected allyl-Pd/**L11** complex (**int-2**) was formed as the major species in the reaction.

Finally, evaluation of the solubility of the potassium salt of the malonate, which would be generated from reaction of the cleaved malonate and KO<sup>t</sup>Bu, showed that its solubility in the ethylbenzene solvent was low ( $S < 1.6 \times 10^{-5}$  M). This value is consistent with our observation that the solution gradually turned from clear to cloudy as the reaction progressed (Scheme 4H). To confirm the identity of the precipitate, the model reaction was conducted under standard conditions, and the corresponding malonate potassium salt was isolated and identified and collected in about 80% yield (Scheme 4I). Thus, such an intriguing concentration-control pathway facilitated the formation of the C–N bond.

These data are all consistent with the mechanism shown in Scheme 5. The alkene **1a** first binds to the low-valent Pd(0) containing the chiral ligand to provide the Pd-alkene

## Scheme 5. Proposed Mechanism



complexes **int-1** and **int-1'**, which then undergo oxidative addition to form the same matched Pd-allyl complex **int-2**. In this process, exchange of the malonate anion with the anion of KBAr<sup>F</sup><sub>4</sub> produces the potassium salt of the malonate, which precipitates from the nonpolar reaction solvent. Rate-limiting nucleophilic attack of the allyl complex **int-2** by morpholine affords the allyl ammonium **int-3**, which forms the product after deprotonation, and regenerates the Pd(0) catalyst.

## CONCLUSION

In conclusion, an asymmetric amination of a set of unstrained C(sp<sup>3</sup>)–C(sp<sup>3</sup>) bonds has been achieved. In this process, an unstrained alkyl C–C bond is replaced by a thermodynamically less stable C–N bond in moderate to good yields with high enantioselectivities driven by the exclusion of the malonate anion from solution. The C–C amination occurs with several classes of amines, and its synthetic value is illustrated by its application to the concise stereoselective synthesis of an HDAC inhibitor. With the combination of a Tsuji-Trost reaction and a C–C  $\sigma$  bond amination, a simple two-step resolution of a racemic allyl amine to the corresponding enantioenriched allylic amine was also achieved. Mechanistic studies show that the transformation occurs by rate-limiting C–N bond formation and is driven thermodynamically by the low solubility of the cleaved alkyl salt in a nonpolar solvent.

## ASSOCIATED CONTENT

### Supporting Information

The Supporting Information is available free of charge at <https://pubs.acs.org/doi/10.1021/jacs.4c11802>.

Experimental procedures for all reactions and characterization data for all products, including <sup>1</sup>H NMR, <sup>13</sup>C NMR, <sup>19</sup>F NMR, and <sup>31</sup>P NMR spectra (PDF)

## AUTHOR INFORMATION

### Corresponding Authors

John F. Hartwig – Department of Chemistry, University of California, Berkeley, California 94720, United States;

orcid.org/0000-0002-4157-468X; Email: jhartwig@berkeley.edu

**Zhi-Tao He** – State Key Laboratory of Organometallic Chemistry, Shanghai Institute of Organic Chemistry, University of Chinese Academy of Sciences, Shanghai 200032, China; School of Chemistry and Materials Science, Hangzhou Institute for Advanced Study, University of Chinese Academy of Sciences, Hangzhou 310024, China; Ningbo Zhongke Creation Center of New Materials, Ningbo 315899, China; orcid.org/0000-0003-2375-9557; Email: hezt@sioc.ac.cn

## Authors

**Yang Liu** – State Key Laboratory of Organometallic Chemistry, Shanghai Institute of Organic Chemistry, University of Chinese Academy of Sciences, Shanghai 200032, China

**Ye-Wei Chen** – State Key Laboratory of Organometallic Chemistry, Shanghai Institute of Organic Chemistry, University of Chinese Academy of Sciences, Shanghai 200032, China; Department of Chemistry, University of California, Berkeley, California 94720, United States

**Yuan-Xiang Yang** – State Key Laboratory of Organometallic Chemistry, Shanghai Institute of Organic Chemistry, University of Chinese Academy of Sciences, Shanghai 200032, China

Complete contact information is available at:

<https://pubs.acs.org/10.1021/jacs.4c11802>

## Notes

The authors declare no competing financial interest.

## ACKNOWLEDGMENTS

Z.-T.H. acknowledges the National Natural Science Foundation of China (22071262, 22371292), Ningbo Natural Science Foundation (2023J036), Science and Technology Commission of Shanghai Municipality (22ZR1475200), Strategic Priority Research Program of the Chinese Academy of Sciences (XDB0610000), State Key Laboratory of Organometallic Chemistry, and Shanghai Institute of Organic Chemistry for financial support. J.F.H. acknowledges financial support from NIH grant (1R35GM130387).

## REFERENCES

- (1) Rybtchinski, B.; Milstein, D. Metal insertion into C–C bonds in solution. *Angew. Chem., Int. Ed.* **1999**, *38*, 870–883.
- (2) Soullart, L.; Cramer, N. Catalytic C–C bond activations via oxidative addition to transition metals. *Chem. Rev.* **2015**, *115*, 9410–9464.
- (3) Fumagalli, G.; Stanton, S.; Bower, J. F. Recent methodologies that exploit C–C single-bond cleavage of strained ring systems by transition metal complexes. *Chem. Rev.* **2017**, *117*, 9404–9432.
- (4) Xia, Y.; Dong, G. Temporary or removable directing groups enable activation of unstrained C–C bonds. *Nat. Rev. Chem.* **2020**, *4*, 600–614.
- (5) McDonald, T. R.; Mills, L. R.; West, M. S.; Rousseaux, S. A. L. Selective carbon–carbon bond cleavage of cyclopropanols. *Chem. Rev.* **2021**, *121*, 3–79.
- (6) Wang, J.-H.; Blaszczyk, S. A.; Li, X.-X.; Tang, W.-P. Transition metal-catalyzed selective carbon–carbon bond cleavage of vinylcyclopropanes in cycloaddition reactions. *Chem. Rev.* **2021**, *121*, 110–139.

(7) Cohen, Y.; Cohen, A.; Marek, I. Creating stereocenters within acyclic systems by C–C bond cleavage of cyclopropanes. *Chem. Rev.* **2021**, *121*, 140–161.

(8) Murakami, M.; Ishida, N. Cleavage of carbon–carbon  $\sigma$ -bonds of four-membered rings. *Chem. Rev.* **2021**, *121*, 264–299.

(9) Nanda, T.; Fastheem, M.; Linda, A.; Pati, B. V.; Banjare, S. K.; Biswal, P.; Ravikumar, P. C. Recent advancement in palladium-catalyzed C–C bond activation of strained ring systems: Three- and four-membered carbocycles as prominent C3/C4 building blocks. *ACS Catal.* **2022**, *12*, 13247–13281.

(10) Song, F.-J.; Wang, B.-Q.; Shi, Z.-J. Transition-metal-catalyzed C–C bond formation from C–C activation. *Acc. Chem. Res.* **2023**, *56*, 2867–2886.

(11) Liang, Y.-F.; Bilal, M.; Tang, L.-Y.; Wang, T.-Z.; Guan, Y.-Q.; Cheng, Z.-R.; Zhu, M.-H.; Wei, J.-L.; Jiao, N. Carbon–carbon bond cleavage for late-stage functionalization. *Chem. Rev.* **2023**, *123*, 12313–12370.

(12) Pirenne, V.; Muriel, B.; Waser, J. Catalytic enantioselective ring-opening reactions of cyclopropanes. *Chem. Rev.* **2021**, *121*, 227–263.

(13) Bi, X.; Zhang, Q.; Gu, Z. Transition-metal-catalyzed carbon carbon bond activation in asymmetric synthesis. *Chin. J. Chem.* **2021**, *39*, 1397–1412.

(14) Yan, H.; Smith, G. S.; Chen, F.-E. Recent advances using cyclopropanols and cyclobutanols in ring-opening asymmetric synthesis. *Green Synth. Catal.* **2022**, *3*, 219–226.

(15) Matsumura, S.; Maeda, Y.; Nishimura, T.; Uemura, S. Palladium-catalyzed asymmetric arylation, vinylation, and allenylation of *tert*-cyclobutanols via enantioselective C–C bond cleavage. *J. Am. Chem. Soc.* **2003**, *125*, 8862–8869.

(16) Wender, P. A.; Haustedt, L. O.; Lim, J.; Love, J. A.; Williams, T. J.; Yoon, J.-Y. Asymmetric catalysis of the [5 + 2] cycloaddition reaction of vinylcyclopropanes and  $\pi$  systems. *J. Am. Chem. Soc.* **2006**, *128*, 6302–6303.

(17) Matsuda, T.; Shigeno, M.; Makino, M.; Murakami, M. Asymmetric synthesis of 3,4-dihydrocoumarins by rhodium-catalyzed reaction of 3-(2-hydroxyphenyl)cyclobutanones. *J. Am. Chem. Soc.* **2007**, *129*, 12086–12087.

(18) Seiser, T.; Cramer, N. Enantioselective C–C bond activation of allenyl cyclobutanes: Access to cyclohexenones with quaternary stereogenic centers. *Angew. Chem., Int. Ed.* **2008**, *47*, 9294–9297.

(19) Kleinbeck, F.; Toste, F. D. Gold(I)-catalyzed enantioselective ring expansion of allenylcyclopropanols. *J. Am. Chem. Soc.* **2009**, *131*, 9178–9179.

(20) Shintani, R.; Nakatsu, H.; Takatsu, K.; Hayashi, T. Rhodium-Catalyzed Asymmetric [5+2] Cycloaddition of Alkyne–Vinylcyclopropanes. *Chem.–Eur. J.* **2009**, *15*, 8692–8694.

(21) Moran, J.; Smith, A. G.; Carris, R. M.; Johnson, J. S.; Krische, M. J. Polarity inversion of donor–acceptor cyclopropanes: Disubstituted  $\delta$ -lactones via enantioselective iridium catalysis. *J. Am. Chem. Soc.* **2011**, *133*, 18618–18621.

(22) Waibel, M.; Cramer, N. Desymmetrizations of *meso-tert*-norbornenols by rhodium(I)-catalyzed enantioselective retro-allylations. *Chem. Commun.* **2011**, *47*, 346–348.

(23) Lin, M.; Kang, G.-Y.; Guo, Y.-A.; Yu, Z.-X. Asymmetric Rh(I)-catalyzed intramolecular [3 + 2] cycloaddition of 1-yne-vinylcyclopropanes for bicyclo[3.3.0] compounds with a chiral quaternary carbon stereocenter and density functional theory study of the origins of enantioselectivity. *J. Am. Chem. Soc.* **2012**, *134*, 398–405.

(24) Xiong, H.; Xu, H.; Liao, S.; Xie, Z.; Tang, Y. Copper-catalyzed highly enantioselective cyclopentannulation of indoles with donor–acceptor cyclopropanes. *J. Am. Chem. Soc.* **2013**, *135*, 7851–7854.

(25) Zhou, X.; Dong, G. Nickel-catalyzed chemo- and enantioselective coupling between cyclobutanones and allenes: Rapid synthesis of [3.2.2] bicycles. *Angew. Chem., Int. Ed.* **2016**, *55*, 15091–15095.

(26) Trost, B. M.; Bai, W.-J.; Hohn, C.; Bai, Y.; Cregg, J. J. Palladium-catalyzed asymmetric allylic alkylation of 3-substituted 1H-indoles and tryptophan derivatives with vinylcyclopropanes. *J. Am. Chem. Soc.* **2018**, *140*, 6710–6717.

- (27) Cheng, Q.; Xie, J.-H.; Weng, Y.-C.; You, S.-L. Pd-catalyzed dearomatization of anthranils with vinylcyclopropanes by [4 + 3] cycloaddition reaction. *Angew. Chem., Int. Ed.* **2019**, *58*, 5739–5743.
- (28) Yang, J.-F.; Sekiguchi, Y.; Yoshikai, N. Cobalt-catalyzed enantioselective and chemodivergent addition of cyclopropanols to oxabicyclic alkenes. *ACS Catal.* **2019**, *9*, 5638–5644.
- (29) Jiang, C.; Wang, L.; Zhang, H.; Chen, P.; Guo, Y.-L.; Liu, G. Enantioselective copper-catalyzed trifluoromethylation of benzylic radicals via ring opening of cyclopropanols. *Chem* **2020**, *6*, 2407–2419.
- (30) Faltracco, M.; van de Vrande, K. N. A.; Dijkstra, M.; Saya, J. M.; Hamlin, T. A.; Ruijter, E. Palladium-catalyzed cascade to benzoxepins by using vinyl-substituted donor–acceptor cyclopropanes. *Angew. Chem., Int. Ed.* **2021**, *60*, 14410–14414.
- (31) Bitai, J.; Nimmo, A. J.; Slawin, A. M. Z.; Smith, A. D. Cooperative palladium/isothiourea catalyzed enantioselective formal (3 + 2) cycloaddition of vinylcyclopropanes and  $\alpha,\beta$ -unsaturated esters. *Angew. Chem., Int. Ed.* **2022**, *61*, No. e202202621.
- (32) Adhikari, A. S.; Pandit, S.; Kant, R.; Majumdar, N. Iridium-catalyzed enantioselective allylic substitution of vinylcyclopropanes by carboxylic acids. *ACS Catal.* **2023**, *13*, 6261–6267.
- (33) Xiao, Y.-Q.; Li, M.-M.; Zhou, Z.-X.; Li, Y.-J.; Cao, M.-Y.; Liu, X.-P.; Lu, H.-H.; Rao, L.; Lu, L.-Q.; Beauchemin, A. M.; et al. Taming chiral quaternary stereocenters via remote H-bonding stereoreinduction in palladium-catalyzed (3 + 2) cycloadditions. *Angew. Chem., Int. Ed.* **2023**, *62*, No. e202212444.
- (34) Wang, T.-H.; Wang, M.-Y.; Wang, Y.-D.; Li, M.-J.; Zheng, Y.; Chen, Q.-W.; Zhao, Y.; Shi, Z.-Z. Ligand cooperativity enables highly enantioselective C–C  $\sigma$ -bond hydroboration of cyclopropanes. *Chem* **2023**, *9*, 130–142.
- (35) Cao, J.; Wu, H.; Wang, Q.; Zhu, J. C–C bond activation enabled by dyotropic rearrangement of Pd(IV) species. *Nat. Chem.* **2021**, *13*, 671–676.
- (36) Wen, L.; Ding, J.; Duan, L.; Wang, S.; An, Q.; Wang, H.; Zuo, Z. Multiplicative enhancement of stereoenrichment by a single catalyst for deracemization of alcohols. *Science* **2023**, *382*, 458–464.
- (37) Trost, B. M.; Van Vranken, D. L. Asymmetric transition metal-catalyzed allylic alkylations. *Chem. Rev.* **1996**, *96*, 395–422.
- (38) Helmchen, G.; Pfaltz, A. Phosphinooxazolines—a new class of versatile, modular *P,N*-ligands for asymmetric catalysis. *Acc. Chem. Res.* **2000**, *33*, 336–345.
- (39) Trost, B. M.; Crawley, M. L. Asymmetric transition-metal-catalyzed allylic alkylations: Applications in total synthesis. *Chem. Rev.* **2003**, *103*, 2921–2943.
- (40) Lu, Z.; Ma, S. Metal-catalyzed enantioselective allylation in asymmetric synthesis. *Angew. Chem., Int. Ed.* **2008**, *47*, 258–297.
- (41) Springer *Transition metal catalyzed enantioselective allylic substitution in organic synthesis in Topics in organometallic chemistry* Kazmaier, U. Ed.; Springer, Heidelberg: 2012 Vol. 38
- (42) Lumbroso, A.; Cooke, M. L.; Breit, B. Catalytic asymmetric synthesis of allylic alcohols and derivatives and their applications in organic synthesis. *Angew. Chem., Int. Ed.* **2013**, *52*, 1890–1932.
- (43) Butt, N. A.; Zhang, W. Transition metal-catalyzed allylic substitution reactions with unactivated allylic substrates. *Chem. Soc. Rev.* **2015**, *44*, 7929–7967.
- (44) Huang, H.-M.; Bellotti, P.; Glorius, F. Transition metal-catalyzed allylic functionalization reactions involving radicals. *Chem. Soc. Rev.* **2020**, *49*, 6186–6197.
- (45) Pàmies, O.; Margalef, J.; Cañellas, S.; James, J.; Judge, E.; Guiry, P. J.; Moberg, C.; Bäckvall, J.-E.; Pfaltz, A.; Pericás, M. A.; Diéguez, M. Recent advances in enantioselective Pd-catalyzed allylic substitution: From design to applications. *Chem. Rev.* **2021**, *121*, 4373–4505.
- (46) Hartwig, J. F.; Stanley, L. M. Mechanistically driven development of iridium catalysts for asymmetric allylic substitution. *Acc. Chem. Res.* **2010**, *43*, 1461–1475.
- (47) Cheng, Q.; Tu, H. F.; Zheng, C.; Qu, J. P.; Helmchen, G.; You, S. L. Iridium-catalyzed asymmetric allylic substitution reactions. *Chem. Rev.* **2019**, *119*, 1855–1969.
- (48) Rössler, S. L.; Petrone, D. A.; Carreira, E. M. Iridium-catalyzed asymmetric synthesis of functionally rich molecules enabled by (phosphoramidite,olefin) ligands. *Acc. Chem. Res.* **2019**, *52*, 2657–2672.
- (49) Turnbull, B. W. H.; Evans, P. A. Asymmetric rhodium-catalyzed allylic substitution reactions: Discovery, development and applications to target-directed synthesis. *J. Org. Chem.* **2018**, *83*, 11463–11479.
- (50) Süsse, L.; Stoltz, B. M. Enantioselective formation of quaternary centers by allylic alkylation with first-row transition-metal catalysts. *Chem. Rev.* **2021**, *121*, 4084–4099.
- (51) Alexakis, A.; Bäckvall, J. E.; Krause, N.; Pamies, O.; Diéguez, M. Enantioselective copper-catalyzed conjugate addition and allylic substitution reactions. *Chem. Rev.* **2008**, *108*, 2796–2823.
- (52) Nilsson, Y. I.; Andersson, P. G.; Bäckvall, J.-E. Example of the thermodynamic control in palladium-catalyzed allylic alkylation. Evidence for palladium-assisted allylic carbon-carbon bond cleavage. *J. Am. Chem. Soc.* **1993**, *115*, 6609–6613.
- (53) Bricout, H.; Carpentier, J.-F.; Mortreux, A. Further developments in metal-catalyzed C–C bond cleavage in allylic dimethyl malonate derivatives. *Tetrahedron Lett.* **1997**, *38*, 1053–1056.
- (54) Nečas, D.; Turský, M.; Katora, M. Catalytic deallylation of allyl- and diallylmalonates. *J. Am. Chem. Soc.* **2004**, *126*, 10222–10223.
- (55) Sumida, Y.; Yorimitsu, H.; Oshima, K. Nickel-catalyzed arylytic ring-opening of 3-methylenecycloalkane-1,1-dicarboxylates. *Org. Lett.* **2010**, *12*, 2254–2257.
- (56) Clavier, H.; Giordano, L.; Tenaglia, A. Palladium-mediated phosphine-dependent chemoselective bisallylic alkylation leading to spirocarbocycles. *Angew. Chem., Int. Ed.* **2012**, *51*, 8648–8651.
- (57) Higashida, K.; Smail, V.; Nagae, H.; Carpentier, J.-F.; Mashima, K. Nickel-catalyzed asymmetric allylic alkylation of  $\beta$ -dicarbonyl compounds via C–C bond activation of 2-allylated cyclic 1,3-diketones. *ACS Catal.* **2023**, *13*, 2156–2161.
- (58) Chen, Y.-W.; Qiu, Y.; Liu, Y.; Lin, G.-Q.; Hartwig, J. F.; He, Z.-T. Intermolecular asymmetric functionalization of unstrained  $C(sp^3)$ – $C(sp^3)$  bonds in allylic substitution reactions. *Nat. Synth.* **2024**, *3*, 1011–1020.
- (59) Zhao, X. H.; Liu, D. L.; Guo, H.; Liu, Y. G.; Zhang, W. B. C–N bond cleavage of allylic amines via hydrogen bond activation with alcohol solvents in Pd-catalyzed allylic alkylation of carbonyl compounds. *J. Am. Chem. Soc.* **2011**, *133*, 19354–19357.
- (60) Li, M.-B.; Wang, Y.; Tian, S.-K. Regioselective and stereospecific cross-coupling of primary allylic amines with boronic acids and boronates through palladium-catalyzed C–N bond cleavage. *Angew. Chem., Int. Ed.* **2012**, *51*, 2968–2971.
- (61) Li, M.-B.; Li, H.; Wang, J.; Liu, C.-R.; Tian, S.-K. Catalytic stereospecific alkylation of malononitriles with enantioenriched primary allylic amine. *Chem. Commun.* **2013**, *49*, 8190–8192.
- (62) Yu, H.; Zhang, G.; Huang, H. Palladium-catalyzed dearomative cyclocarbonylation by C–N bond activation. *Angew. Chem., Int. Ed.* **2015**, *54*, 10912–10916.
- (63) Xu, Y.-N.; Zhu, M.-Z.; Tian, S.-K. Chiral  $\alpha$ -amino acid/palladium-catalyzed asymmetric allylation of  $\alpha$ -branched  $\beta$ -ketoesters with allylic amines: Highly enantioselective construction of all-carbon quaternary stereocenters. *J. Org. Chem.* **2019**, *84*, 14936–14942.
- (64) Angibaud, P.; et al. Identification of a series of substituted 2-piperazinyl-5-pyrimidylhydroxamic acids as potent histone deacetylase inhibitors. *Bioorg. Med. Chem. Lett.* **2010**, *20*, 294–298.